

**Effect of Heat Treatment on Magnetic and Mechanical Properties of
an Iron-Cobalt-Vanadium-Niobium Alloy.**

Benjamin T. Hailer

Thesis submitted to the Faculty of Virginia Polytechnic Institute and State
University as partial fulfillment of the requirements for the degree of

Master of Science

in

Materials Science and Engineering

Steven L. Kampe, Co-Chair

William T. Reynolds, Jr., Co-Chair

Alex O. Aning

Richard T. Fingers

December 3, 2001

Blacksburg, Virginia

Keywords: Iron Cobalt alloy, Hipercor 50HS, magnetic, mechanical

Effect of Heat Treatment on Magnetic and Mechanical Properties of an Iron-Cobalt-Vanadium-Niobium Alloy.

Benjamin T. Hailer

(Abstract)

Iron-cobalt-vanadium alloys can be processed to have excellent soft magnetic properties for use in high performance power generation applications such as the rotors and stators of aircraft integrated power units. These soft magnetic properties are, however, developed at the expense of mechanical strength and toughness. Small additions of niobium are reported to increase the strength of these Fe-Co-V alloys. This study evaluates the effects of heat treatment on the mechanical and magnetic properties of heavily cold work strip of a 48 wt.% iron-48 wt.% cobalt-2 wt.% vanadium alloy with a 0.3 wt.% addition of niobium.

For heat treatments between 640 and 740°C for 1 hour the tensile and yield strengths and ductility of the alloy were all found to be superior to a similar alloy found in the literature without the addition of Nb and processed in a similar manner. Magnetic permeability, remnant induction, saturation induction, coercivity and core loss were only slightly degraded at all annealing temperatures when compared with the non-niobium containing alloy. All properties were shown to depend primarily on degree of recrystallization of the sample, which was found to fully recrystallize between 720 and 740 °C for 1 hour anneals. No significant change in measured properties were found when annealing time was increased to 2 hours. Full recrystallization was observed for samples annealed for as short of times as 10 minutes at 800 °C.

Table of Contents:

Abstract.....	i
Table of Contents:	ii
List of Figures	iii
List of Tables:.....	iv
Introduction	1
Experimental Procedure	5
Results and Discussion.....	7
Conclusions	16
References	18
Vita.....	19

List of Figures:

Figure 1: Typical magnetic hysteresis loop.....	2
Figure 2: Ternary and pseudo-binary phase diagrams for the Fe-Co-V system.	3
Figure 3: Data from a ternary Fe-Co-V alloy.....	5
Figure 4: Some typical stress-strain curves showing yield point elongation.	6
Figure 5: Elongation of Hiperco 50HS annealed for 1 hour	8
Figure 6: Microstructure of Hiperco 50 HS after 1 hour anneal at 680 °C.	9
Figure 7: Microstructure of Hiperco 50 HS after 1 hour anneal at 720 °C	9
Figure 8: Microstructure of Hiperco 50 HS after 1 hour anneal at 740 °C	10
Figure 9: The yield and tensile strengths of Hiperco 50HS, 1 hour anneal	12
Figure 10: Initial and maximum magnetic permeability of Hiperco 50HS annealed for 1hr.	13
Figure 11: Increase in remnant induction of Hiperco 50HS, annealed for 1hr and tested to a maximum applied field of 20 Oe cycled at 60 Hz.....	14
Figure 12: Coercivity of Hiperco 50HS annealed for 1hr and tested under a maximum applied field of 20 Oe. cycled at 60 Hz.....	15
Figure 13: Full loop core loss at 60 Hz for Hiperco 50HS annealed for 1 hour.	16

List of Tables:

Table I: Times and temperatures used for annealing treatments.....6
Table II: Elemental composition of several γ_2 particles from various heat treatments analyzed by
EDS.....11

Introduction

The rotors in integrated electrical power units and internal starter/generators for main propulsion aircraft engines require a material with a combination of soft magnetic properties and high mechanical strength. To function as a magnetic core, the rotor material must have a high magnetization to effectively concentrate magnetic field lines. Because spinning rotors are subjected to rapidly changing magnetic fields, they also must be magnetically soft, or capable of being magnetized and demagnetized easily. From the point of view of mechanical behavior, rotors require enough strength to support the centrifugal stresses generated at high rotational speeds. These magnetic and mechanical property requirements are difficult to achieve simultaneously. The microstructural strategies that increase strength by impeding dislocation motion also tend to impede the motion of magnetic domain walls necessary for magnetization and demagnetization during use.

Several parameters give useful information for evaluating a material's soft magnetic performance. The properties commonly used to characterize soft magnetic materials reflect the engineering requirements of generator applications and can be seen graphically when the induced magnetization of a material driven to saturation first in one direction, then in the opposite direction, then back to the original direction is plotted against the external applied field. Permeability is a measure of a material's susceptibility to magnetize in response to an applied magnetic field. Permeability, μ , is the slope of a straight line drawn between the origin of the initial B-H curve, seen in Figure 1, to some desired level of magnetization, such as saturation. Remnant induction, B_r , indicates the extent to which the material remains magnetized after the applied magnetic field is removed and can be seen on a hysteresis loop as the induction when zero field is applied. Coercivity, H_c , is the strength of the opposing magnetic field required to drive the magnetization of a fully magnetized sample back to zero, it can be seen where the external field value of the hysteresis loop crosses the H axis. It provides information about the difficulty of moving domain walls, and it is highly sensitive to microstructure. Finally, core loss is a measure of the energy expended during a magnetization cycle. Core loss reflects all the eddy current losses in a magnetic core material induced by the alternating magnetic field in the generator. Barriers to smooth domain wall motion and rotation increase core loss, so

microstructure tends to have a similar effect on core loss and coercivity. Core loss is directly proportional to the area of the hysteresis loop.

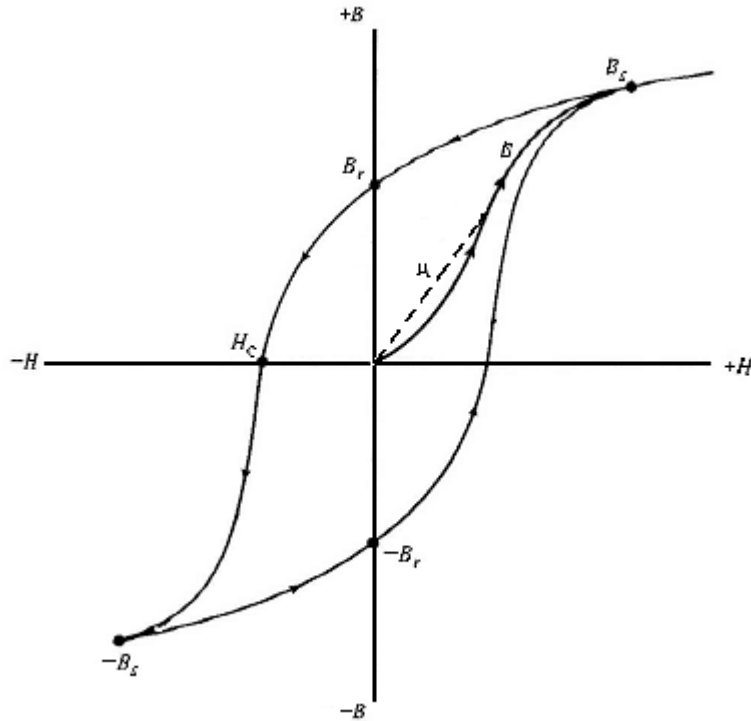


Figure 1: Typical magnetic hysteresis loop illustrating the origin of several key magnetic parameters.

Weight is also a critical factor in aircraft generators, and this consideration has focused interest upon Fe-Co alloys. This class of alloys combines the highest saturation magnetizations found in ferromagnetic materials, high permeability, and enough strength to withstand rotational stresses^{1, 2, 4}. Equiatomic Fe-Co alloys have high strength as well as relatively low coercivity and moderate core loss but are brittle, and difficult to roll into sheet for generator cores. However, the addition of 2 wt % vanadium produces an alloy with acceptable ductility without significantly affecting the strength, only slightly lowering the saturation magnetization and permeability, and slightly increasing the coercivity³.

Many of the salient structure and property characteristics of the Fe-Co-base alloys are summarized in Bozorth⁴ and in a review by Couto and Ferreira⁵. Upon cooling to 980 °C, near

equiatomic Fe-Co changes from a paramagnetic γ phase (fcc) to the ferromagnetic α phase (bcc). Below 730 °C, the α phase transforms to the ordered, α' phase (B₂ structure). The addition of 2% V serves to widen the two-phase $\alpha + \gamma$ region enough that α and γ are stable even down to room temperature.⁶ It also retards the kinetics of the ordering reaction below 730°C. This ordering transition occurs very rapidly in the equiatomic alloy, but the presence of V suppresses ordering during rapid quenching.⁷

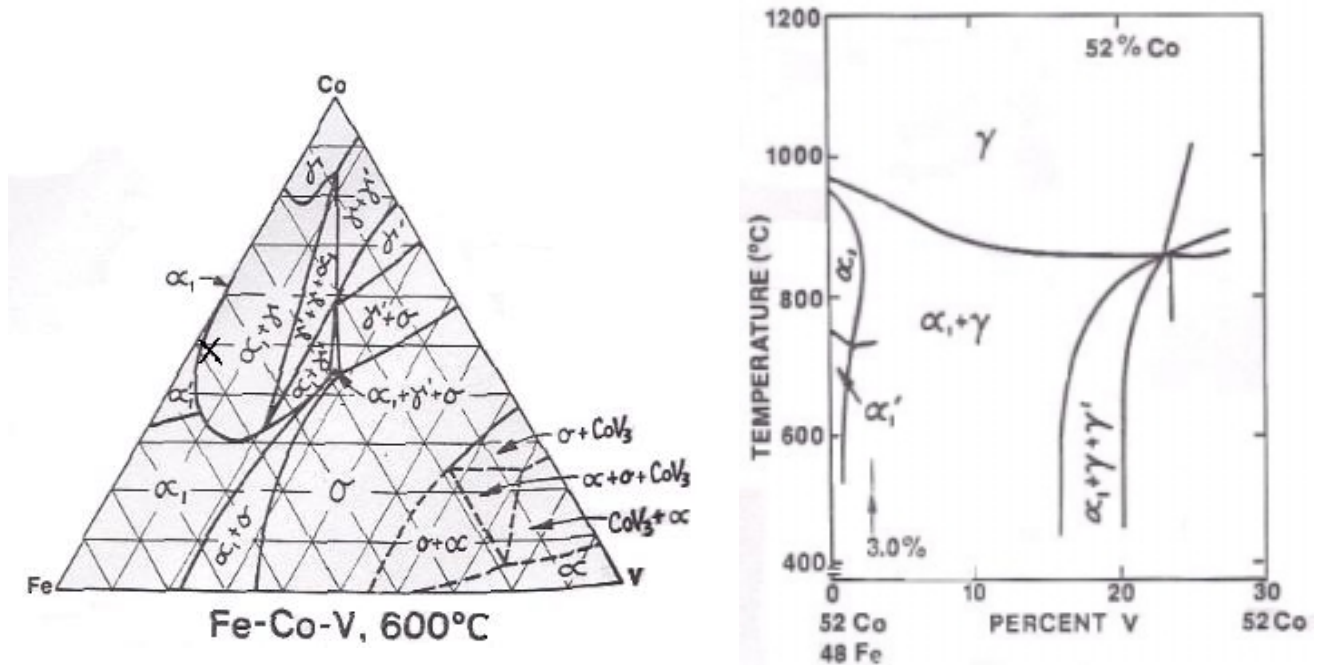


Figure 2: Ternary and pseudo-binary phase diagrams for the iron-cobalt-vanadium system.⁸ Marks indicate the approximate composition Hiperco 50HS.

While it is relatively clear that the presence of the ordered α' phase does not significantly affect the strength, it does lower ductility in the alloy. Kawahara found that significant ductility can be retained in alloys with high degrees of long range order provided the alloy was previously cold rolled with a reduction of at least 72%⁹. Kawahara systematically examined samples heat treated from both cold worked and cast and quenched alloys and concluded that the higher ductility in cold rolled alloys was most likely caused by elongated strands of metastable γ_2 phase (fcc). These γ_2 particles, the presence of which was noted in other investigations,^{10, 11, 12} are found to make up about 2 wt. % of the alloy and have been identified as fcc Co_3V with some substitution of Fe atoms for V.¹¹ One explanation for why these particles lead to increased ductility is that

they locally deplete the surrounding alloy of Co, and in doing so suppress the formation of the ordered α' structure. The resulting structure is similar to a fiber-reinforced composite with a matrix phase of ordered α' and “fibers” running parallel to the rolling direction of the material consisting of more ductile regions of γ_2 surrounded by disordered α . The γ_2 particles provide an additional contribution to mechanical strengthening because they tend to precipitate on grain boundaries in heavily cold worked alloys and act as grain refiners during subsequent heat treatments. They thus refine the grain size and increase strength through a Hall-Petch relationship.¹³

The γ and γ_2 phases have little effect on the saturation magnetization because this property depends upon the volume fraction of the ferromagnetic phase, and the amount of the (paramagnetic) γ and γ_2 phases present is relatively small. However, the γ and γ_2 particles, as well as the reduced α grain size they induce, have an undesirable effect on the coercivity and the core loss. These properties increase with the resistance to domain wall motion, and both paramagnetic inclusions (the γ and γ_2 phases) and grain boundaries are effective at pinning domain walls. Consequently, increasing the strength of Fe-Co-V alloys is achieved at the expense of magnetic performance. For this reason, Fe-Co-V alloys for rotor applications need to be heat treated to produce a microstructure that strikes a balance between the strength needed to withstand rotational stresses and the low coercivity needed to minimize core loss.

Recent work has been done on quaternary alloys of Fe-Co-V-X where X represents intentional additions of nickel, carbon, chromium, yttrium, niobium, molybdenum, tantalum, or tungsten.^{14, 15, 16} Like Fe-Co-V, these alloys were found to form intermetallic compounds of the form Co_3X . In this study, we investigate the properties of Hiperco 50HS[®], an Fe-Co-2V-0.3 Nb alloy produced by Carpenter Technology Corporation (Reading, PA). Specifically, we measure the mechanical and magnetic properties of cold-rolled sheet annealed at a series of times and temperatures.

A study very similar to this was performed by D. R. Thornburg¹⁸ using a ternary alloy with composition 48.3 wt.% Fe, 49.4 wt.% Co, 1.98 wt.% V. Some of the results from this investigation can be seen in Figure 3.

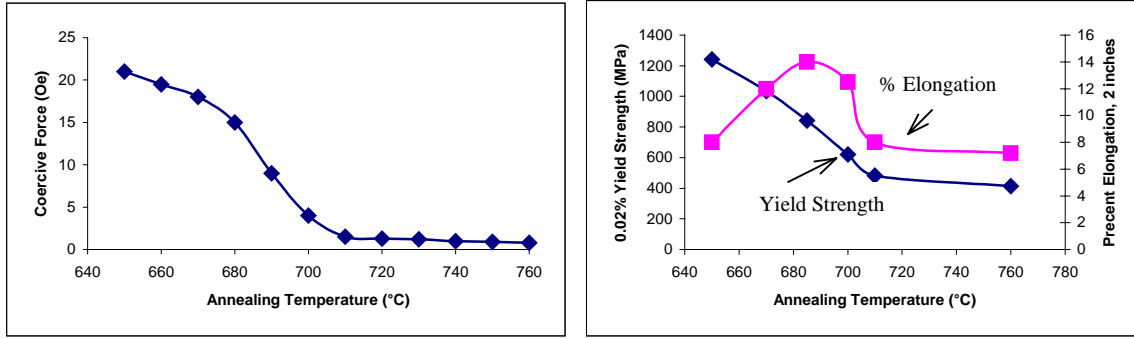


Figure 3: Data from a ternary Fe-Co-V alloy treated much like the material in this study.¹⁸

Experimental Procedure

Samples of Hipercor 50HS, composition 48.62 wt.% Co, 1.91 wt.% V, 0.29 wt.% Nb, 0.04 wt.% Si, 0.03 wt.% Mn, 0.013 wt.% C, and balance Fe, were obtained from Carpenter Specialty Alloys in as-rolled strip form, 0.15 mm nominal thickness. Tensile “dog bone” specimens were machined with the tensile axis oriented 45° to the rolling direction. The specimens had a 25 mm gauge length and a 50.8 mm radius transition from the gauge section to the grip tabs. Because the metal is notch sensitive, this gradual transition from the grip tabs to the gauge section was necessary to insure all the specimens failed within the gauge length. A 45° orientation was chosen because previous studies of this alloy indicated that it was the lowest strength direction.¹⁷ Samples for magnetic testing were rectangular strips, also cut 45° to the rolling direction, 2.5 cm wide by 22.6 cm in length.

Sets of three rectangular strips and three tensile specimens were each annealed in an atmosphere of flowing hydrogen for the times and temperatures indicated in Table I. The samples were inserted into the hot zone of the furnace equilibrated at the annealing temperature, held for the chosen time, and then removed to a cool end of the furnace. Once removed from the hot zone, the sample temperature dropped approximately 250 °C within the first minute.

Table I: Times and temperatures used for annealing treatments.

		Heat Treatment Temperature, °C.								
		640	660	680	700	720	740	760	780	800
Heat Treatment Time (min.)	10								X	X
	30							X	X	X
	60	X	X	X	X	X	X	X	X	X
	120	X	X	X	X	X	X			

The tensile specimens were pulled to failure in an Instron testing frame at an initial strain rate of $6.7 \times 10^{-3} \text{ s}^{-1}$ and the stress-strain behavior recorded. The percent elongation was measured by use of an extensometer within the 1-inch gauge section. This material sometimes exhibits yield point elongation associated with the formation of Lüders bands across the gauge region of the tensile specimen.¹⁷ When yield point elongation occurred, the reported yield strengths were obtained from the intersection of a 0.2% offset plastic strain with the lower yield value. Typical examples of the stress-strain behavior of this material can be seen in Figure 4.

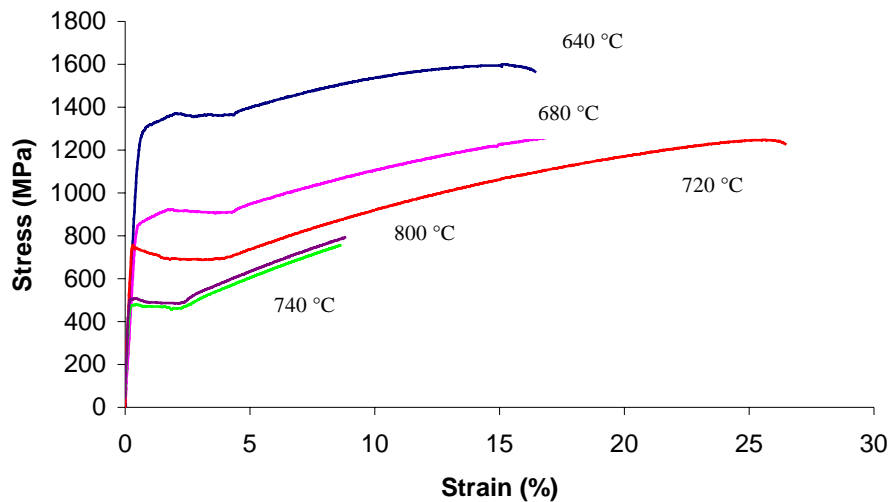


Figure 4: Some typical stress-strain curves showing yield point elongation measured for Hiperco 50 HS annealed for 1 hour at various temperatures.

Room temperature magnetic properties were measured using a Walker Scientific AMH-20 hysteresisgraph and single strip test fixture conforming to ASTM standard test procedure A804.

Both initial induction and full hysteresis loop tests, at 60 Hz to a maximum applied field of 20 and 200 Oe, were performed.

Selected magnetic test specimens were sectioned and mounted such that a plane 45° to the short transverse rolling direction was exposed for metallographic inspection. Final polishing was done using 0.04 μm colloidal silica, and the samples were etched with 15% nital (15 vol% HNO₃ in methanol) for approximately 100 seconds. Successively higher annealing temperatures required longer etching times to achieve the same degree of etch, times as long as 180 seconds were used for the highest annealing temperatures.

Results and Discussion

Figure 5 shows the effect of annealing temperature on tensile ductility (percent elongation at failure) for 1-hour treatments. As no necking was ever observed, the measured elongation represents uniform elongation. The percent elongation data for the samples increased from approximately 16% after a 640 °C anneal to between 20 and 26% at 720°C. The ductility falls quickly to approximately 8% with an increase in annealing temperature of only an additional 20 °C. An examination of the microstructure produced by each annealing treatment revealed that the material recrystallizes at a temperature between 720 and 740 °C, perhaps coincidentally, very close to the temperature at which ordered α' converts to disordered α (see Figures 6,7 and 8). This suggests the precipitous drop in ductility between 720 and 740 °C is associated with the recrystallized condition. Similar trends in ductility have been noted in Fe-Co-V alloys, but the minimum ductility in these studies was reported at conditions just prior to full recrystallization.⁷

18

For anneals below the recrystallization temperature, the deformed grains recover and produce an increase in ductility. Although there is sufficient time to fully order a uniform alloy while annealing below the recrystallization temperature, local concentration depleted regions associated with Co₃X particles should remain effective in suppressing α' and these regions are likely to remain effective contributors to ductility. If the Co₃X particles or the Co depleted regions around them disappear as the alloy recrystallizes, the ductile fiber structure will be lost

and the alloy will be able to transform to the inherently less ductile ordered α' more completely upon cooling.

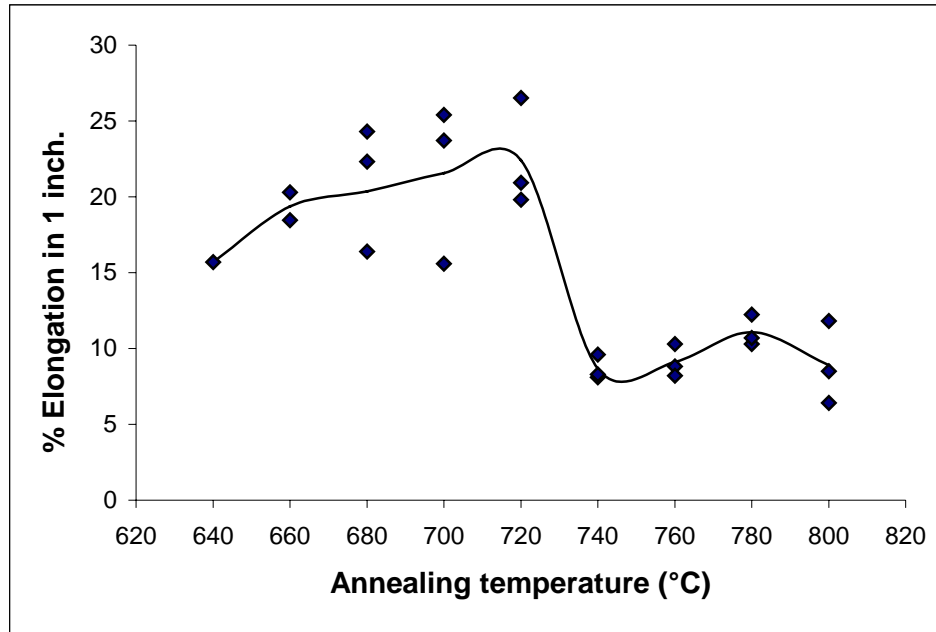


Figure 5: The sharp drop in the elongation of Hiperco 50HS annealed for 1 hour between the 720 and 740°C treatments associated with recrystallization. The continuous line indicates the average value of the data taken at each annealing temperature.

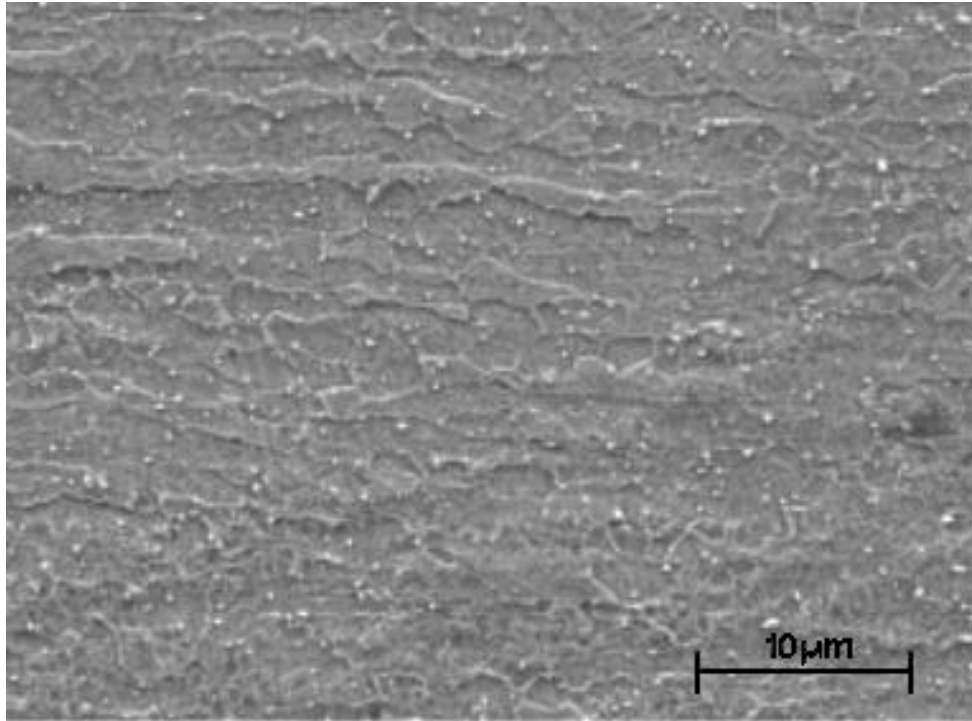


Figure 6: The elongated structure formed during rolling is still present after a 1 hour anneal at 680 °C. Structure is primarily α or α' grains with lighter γ or γ_2 particles dispersed throughout.

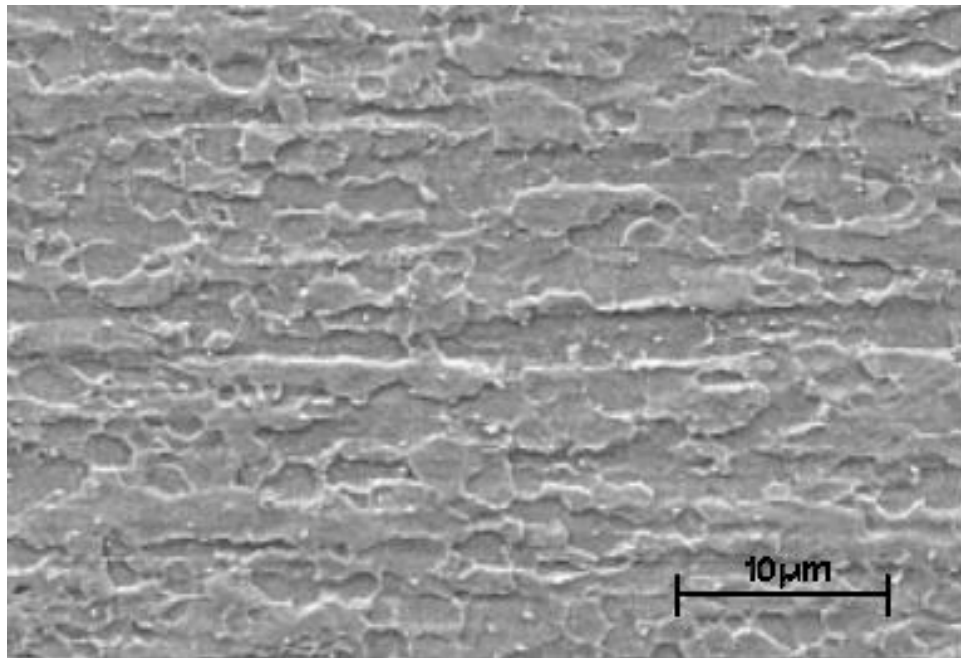


Figure 7: Nucleation of new grains is readily apparent after a 1-hour anneal at 720 °C.

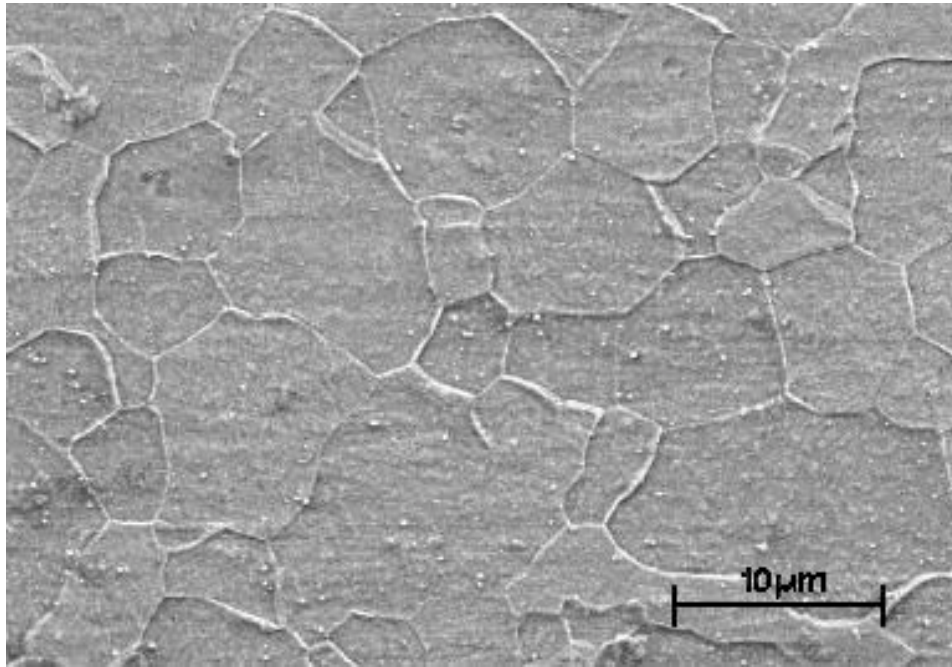


Figure 8: Fully recrystallized microstructure resulting from a 1 hour anneal at 740°C.

An effort was made to determine the compositions of the suspected γ_2 particles seen in the microstructure using a scanning electron microscope for EDS, electron dispersive spectroscopy. The particles are on average about 100 nm in diameter and the minimum spot size for EDS approximately $1 \mu\text{m}^3$ so quite a bit of the matrix enters into the analyzed sample. The results of the analysis of several particles in various heat treatments, Table II, show that the particles are especially elevated in niobium and to a lesser extent cobalt and possibly vanadium while being iron deficient compared to the bulk. If the average particle size is taken to be 10% of the total sample volume, and the rest set to the bulk composition, the concentration of the particle would be 74 wt% Co, 20wt% Nb and 4 wt.% V, very close to a Co_3Nb particle with some vanadium substitution of niobium. While not a conclusive determination of these particles being $\text{Co}_3(\text{Nb},\text{V})$, these results definitely seem to indicate the presence of some phase especially rich in cobalt and niobium with some vanadium.

Table II: Elemental composition of several γ_2 particles from various heat treatments analyzed by EDS.

	Weight Percent				
	Fe	Co	V	Nb	Si
Matrix *	49.1	48.6	1.9	0.3	0.04
Precipitate 1	44.2	51.1	2.1	2.5	0.08
2	44.6	51.2	1.8	2.3	0.05
3	45.7	50.3	2.4	1.3	0.2

* Corrected concentrations using matrix composition equal to overall alloy composition, as determined by manufacturer chemical analysis, as standard.

The tensile properties of the alloy as a function of annealing temperature are shown in Figure 9. Both yield and tensile strength appear to decrease at a similar rate with increasing annealing temperature up to 740°C where both the tensile strength and the yield strength appear to become insensitive to further increase in annealing temperature.

Since elastic modulus is not affected by heat treatment, the modulus values obtained from all the tensile tests were averaged. The average value was 170 ± 10 GPa, well below the value of 207 GPa reported by Carpenter¹⁹. Since all tensile measurements were made at a 45° angle to the rolling direction of the sheet, elastic anisotropy and crystal texture may account for the discrepancy.⁷

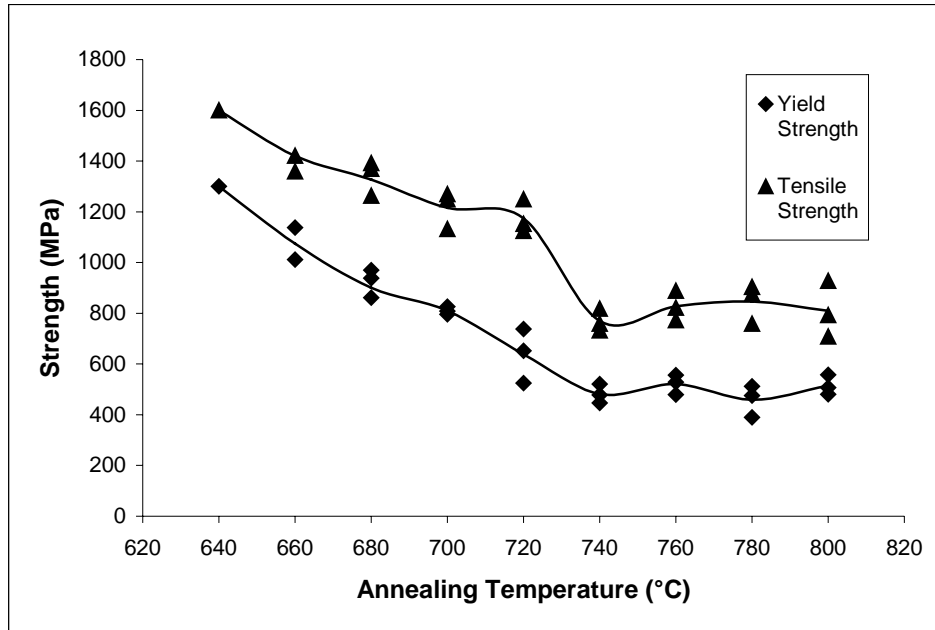


Figure 9: The yield and tensile strengths of Hipercro 50HS decrease steadily with increase in annealing temperature of 1 hour treatments up to the recrystallization temperature, beyond which no significant change is seen.

The initial permeability and maximum permeability as a function of annealing temperature are shown in Figure 10. These quantities were measured from the induction curve obtained using a slowly increasing (as opposed to an alternating) field applied to initially demagnetized samples. Initial permeability is the ratio of the induction to the magnetic field at low fields where the induction varies linearly with the field. In this regime, magnetization occurs primarily by the motion of domain walls. The maximum permeability is the ratio of the induction to the field at the maximum field employed in the test. The induction and field are no longer linear in this regime and changes in magnetization occur by domain rotation. Both types of permeability increase only slightly with annealing temperature below the recrystallization temperature. Above this temperature, both permeabilities increase substantially. For annealing temperatures below 720°C, the partial removal of defects during recovery accounts for the gradual rise in permeability. The abrupt increase at annealing temperatures over 720°C corresponds to the appearance of dislocation-free α or α' grains, and perhaps a reduction in the amount of nonmagnetic γ and γ' inclusions. The later explanation is supported by the observation that the maximum induction at 100 Oe increases smoothly with annealing temperature from 20 kG after the 640°C anneal to a maximum value of 25 kG after the 800 °C, 1 hour anneal. The

comparatively larger increase in the maximum permeability with increasing annealing temperature (above the recrystallization temperature) is attributed to grain growth.

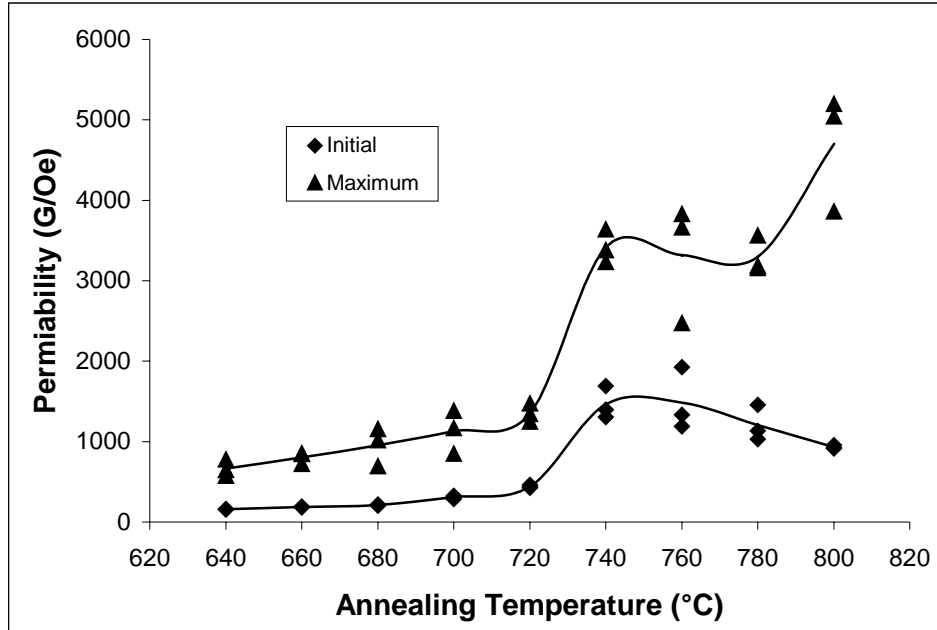


Figure 10: Grain growth after recrystallization likely accounts for the sudden increase in both initial and maximum magnetic permeability of Hiperco 50HS annealed for 1hr.

The remnant induction, shown in Figure 11, appears to increase continuously with annealing temperature up to the recrystallization temperature. Above this, there is little change in the remnance. Remnant induction depends upon the type and amount of ferromagnetic material present and is largely insensitive to microstructure, hence the relatively low amount of increase with annealing temperature when compared with other magnetic properties.

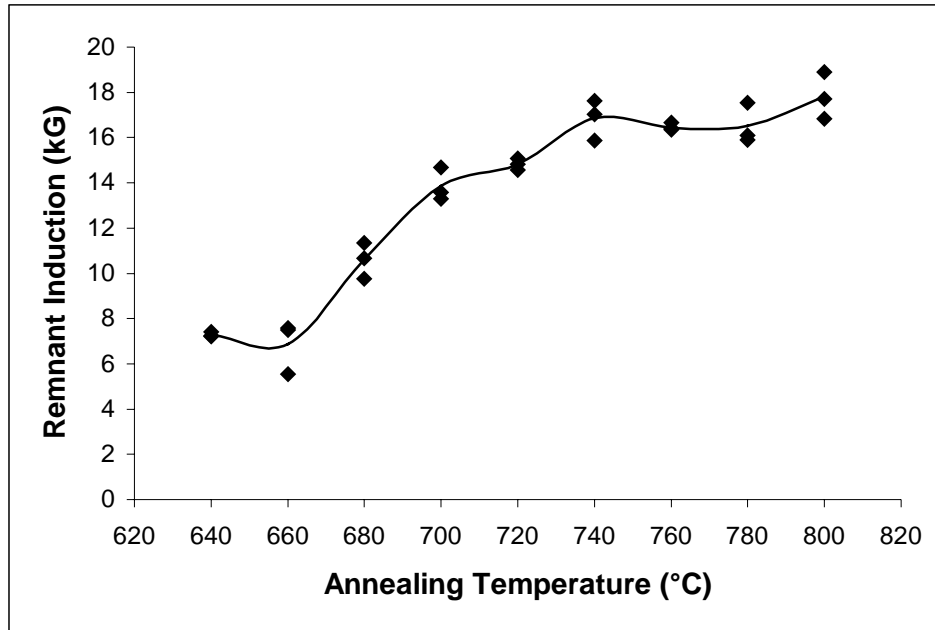


Figure 11: The increase in remnant induction of Hiperco 50HS, annealed for 1hr and tested to a maximum applied field of 20 Oe cycled at 60 Hz, occurs steadily up to the recrystallization temperature and then ceases.

The response of the coercive force to annealing (shown in Figure 12) is typical of soft ferromagnetic alloys. The coercivity decreases with annealing temperature up to the recrystallization temperature and then remains unchanged at higher temperatures. This is primarily because coercivity reflects the presence of impediments to domain wall motion. Fully recrystallized samples have comparatively few imperfections to pin domain walls. The core loss follows a similar trend as the coercivity, Figure 13. The low core loss in the recrystallized condition reflects the relative ease with which magnetic domains move in the larger, defect-free grains. While the core loss measurements with a 20 and 200 Oe fields both reflect the pinning effects of defects remaining after annealing, the measurements made with the higher field are most sensitive to microstructure. This implies the viscous losses arising from eddy current damping (which depend upon applied magnetic field through the domain wall velocity) are also quite structure sensitive.

In addition to the one hour annealing treatments discussed so far, 2 hour annealing treatments at temperatures below 740°C and some shorter duration anneals of 10 and 30 min. at the upper end of the investigated temperature range were also performed. Within the error of the

measurements, there was no significant difference between the 1 and 2 hour anneals with respect to the microstructural, mechanical, or magnetic behavior. The short duration anneals resulted in properties very close to the longer anneals for a given degree of recrystallization. Annealing at 800 °C for 10 and 30 minutes resulted in the same degree of recrystallization and grain size seen after 1 and 2 hour treatments at 800 °C and correspondingly similar measured properties.

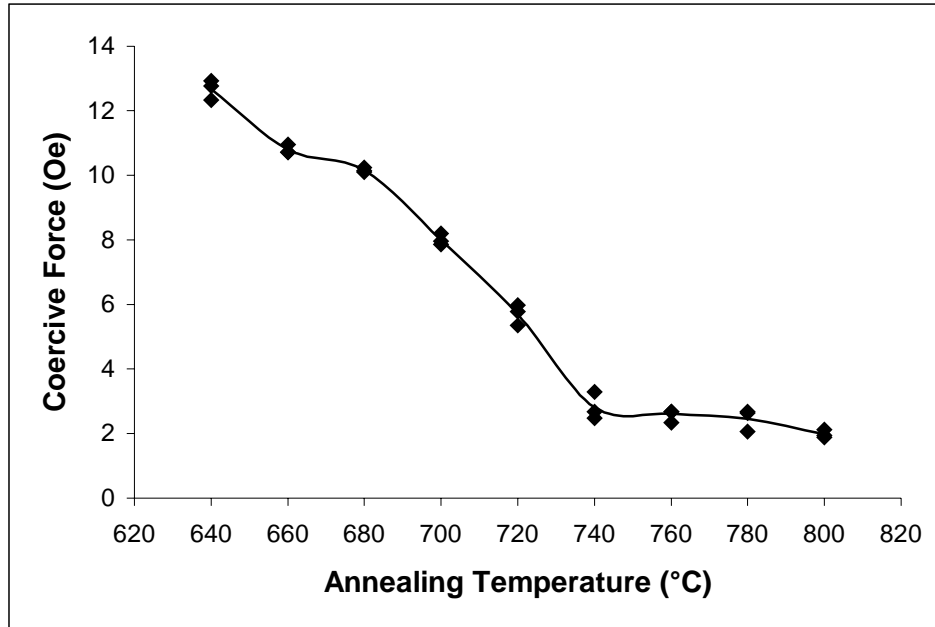


Figure 12: Coercivity depends largely on microstructural features which reach a constant value after recrystallization of the alloy around 730°C. Hiperco 50HS annealed for 1hr and tested under a maximum applied field of 20 Oe, cycled at 60 Hz.

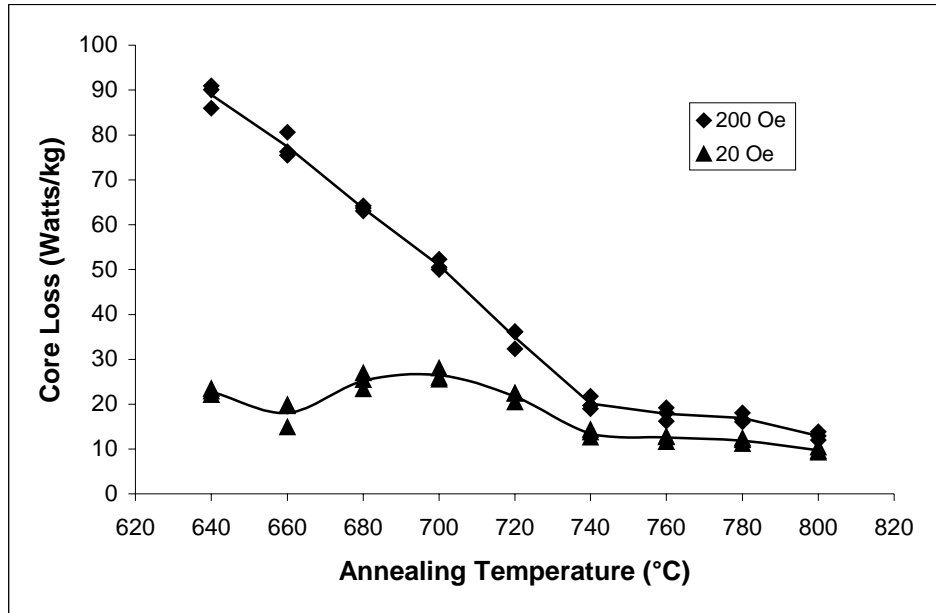


Figure 13: Full loop core loss at 60 Hz, measured using ASTM standard A804. Core loss measured at higher applied fields shows greater sensitivity changes in microstructure prior to recrystallization.

Conclusions

The quaternary alloy of Fe-Co-V-Nb appears in most respects to follow the general behavior of the thoroughly investigated ternary alloy.¹⁸ The full recrystallization temperature for this alloy may be slightly higher, 730 °C for 1 and 2 hours compared with 710 °C for 2 hours as reported by Thornburg.¹⁸ Ductility was found to be significantly higher for intermediate annealing temperatures, when compared against similar alloy compositions without the addition of niobium, but similar once the material had recrystallized. There was an overall improvement in strength over the ternary alloy under all examined annealing conditions. The coercivity and remnant induction¹² were both lower at intermediate annealing conditions, a desirable characteristic for a rotor material, but quite similar to the ternary alloy once in the fully recrystallized state. The saturation magnetization was, for all heat treatment conditions, higher than the values reported for Fe-Co-V.¹⁸

Although still unconfirmed, it is speculated that the Nb addition serves a similar function as V in the ternary alloy by forming metastable fcc precipitates approximately of a composition Co_3Nb . These particles may serve to increase strength by inhibiting α' grain growth and improving

ductility after cold rolling by forming local Co-depleted zones that locally suppress ordering during cooling.

The mechanical properties obtained after annealing at temperatures below the recrystallization temperature appear to benefit from these local Co-depleted zones, but the effect is diminished in fully recrystallized material. It would appear that these precipitates do not have a detrimental effect on the saturation magnetization, coercivity and remnant induction relative to the ternary Fe-Co-V alloy.

Little difference was found when the samples were annealed for times longer than 1 hour and annealing at 800°C for times as short as 10 minutes appear to be sufficient to cause full recrystallization.

References

- ¹ A. Preuss, dissertation, University of Zurich, 1912.
- ² P. Weiss, *Trans. Faraday Soc.* **8**, p. 148, 1912.
- ³ J. H. White and C.V. Wahl, U.S. Patent 1862559, 1932.
- ⁴ R. M. Bozorth, "Ferromagnetism," IEEE Press, Piscataway, NJ, 1951.
- ⁵ A. A. Couto and P. I. Ferreira, *J. Mat. Eng.*, **11**(11), p. 31, 1989.
- ⁶ W. Koster and H. Schmid, *Archiv, Eisenhüttenw.*, **26**, p. 345-53, 1955.
- ⁷ Emile Josso, *IEEE Trans. on Mag.* vol **Mag-10**(2), p. 161, 1974.
- ⁸ W. Köster and H. Schmid: *Archiv, Eisenhüttenw.*, **26**, p. 345-53 and 421-25, 1955.
- ⁹ Kohji Kawahara, *J. of Mat. Sci.* **18**, p. 3437, 1983.
- ¹⁰ R. D. Rawlings, H. M. Flower, and J.A Ashby, *Met. Sci.*, **11**, p. 91, 1977.
- ¹¹ H. C. Fiedler and A. M. Davis, *Met. Trans.* **1**, p. 1036, 1970.
- ¹² M. R. Pinnel and J. E. Bennett, *Met. Trans.*, **5**, p. 1273, 1974.
- ¹³ C. Shang, R. C. Cammarata, T. P. Weihs, C. L. Chien, *J. Mater. Res.* **15**(4), p. 835, 2000.
- ¹⁴ C. D. Pitt and R. D. Rawlings, *Met. Sci.* **17**(6), p. 261, 1983.
- ¹⁵ M. W. Branson, R. V. Major, C. D. Pitt, and R. D. Rawlings, *J. of Magn. And Mag. Mat.* **19**, p. 222, 1980.
- ¹⁶ C. D. Pitt and R. D. Rawlings, *Met. Sci.* **15**, p. 369, 1981.
- ¹⁷ Richard T. Fingers, "Creep Behavior of Thin Laminates of Iron-Cobalt Alloys for use in Switched Reluctance Motors and Generators", Thesis, Virginia Tech, p. 46, 1998.
- ¹⁸ D. R. Thornburg, *J. Applied Physics* **40**(3), p. 1579, 1969.
- ¹⁹ Carpenter Materials Data Sheet, Carpenter Specialty Alloys

Vita**Benjamin T. Hailer**

Born in Weston, West Virginia in 1976. Received a Bachelor's of Science degree in Materials Science and Engineering from Virginia Polytechnic Institute and State University in 1998. Currently employed by NASA Langley as a student trainee working toward a PhD, once again in MSE from Virginia Tech.